



OPEN A streamlined POCT solution for rapid infectious disease detection

Yaping Xie, Yan Yu, Shuaiwu Huang, Liangcheng Wan, Chang Wu, Chiwei Yin, Jianjun Li, Jiangang Ling & Lizhong Dai✉

Point-of-care testing (POCT) plays a crucial role in infectious disease screening due to its rapid detection and portability. However, current POCT systems face challenges such as lengthy sample preparation time, complex nucleic acid extraction, and limited real-time data transmission, extending patient waiting time. This study presents iPonatic, an integrated POCT system with a quantitative dropper for efficient sample addition, a low-cost cartridge utilizing one-step rapid nucleic acid release technology, and real-time data synchronization via a cloud platform. Patients can receive test reports within 30 min. The system was validated for both respiratory and sexually transmitted pathogens, showing consistent Ct values with standard quantitative PCR. Clinical validation on 1159 samples demonstrated an AUC above 0.98 for all targets, with sensitivity exceeding 95% and specificity reaching 100%. iPonatic is ideal for primary healthcare, epidemic response, and resource-limited settings. It offers an efficient solution to enhance diagnostics and reduce patient waiting time, supporting timely responses to public health needs.

Keywords Point-of-care, Quantitative dropper, One-step nucleic acid release technology, iPonatic, Respiratory infection, Sexually transmitted infection

Efficient pathogen detection is crucial for the timely and effective control of infectious diseases. Nucleic acid testing has become widely recognized as the 'gold standard' for pathogen detection due to its high sensitivity and specificity. However, its reliance on laboratory infrastructure, bulky equipment, and skilled personnel limits its applicability in rapid screening and large-scale testing^{1,2}. Point-of-care testing (POCT) technology overcomes the constraints of traditional laboratories, offering simplicity in operation and short turnaround times. It has become a vital tool for infectious disease detection, with significant potential in pandemic emergency responses, remote regions, and primary healthcare settings^{3–8}.

Despite these advantages, existing POCT systems face challenges such as prolonged sample preparation time, complex nucleic acid extraction processes, and limited real-time data transmission capabilities, resulting in low detection efficiency and extended patient waiting time^{9,10}. Specifically, nucleic acid extraction typically uses magnetic beads^{11,12} or silicon materials^{13–15}, which require intricate fluidic systems, leading to high costs and long processing time. Additionally, most systems rely on USB or Bluetooth for short-range data transmission^{16–19}, lacking remote real-time monitoring capabilities. While fully integrated commercial devices, such as GeneXpert^{20,21} and FilmArray²² offer advanced data capabilities, their complex nucleic acid extraction and high per-test costs—ranging from tens to hundreds of dollars²³—make them inaccessible in primary care settings and low-resource regions.

To overcome these limitations and reduce patient waiting time, we developed the iPonatic system, an intelligent POCT system that enhances efficiency and the speed of report generation. Firstly, we developed a quantitative dropper that integrates sample collection and precise dispensing. It features a dispensing capsule design for precise liquid volume control and a cavity for liquid storage. By combining the functions of a reagent storage tube and a pipette, it reduces the need for specialized operation, minimizes the risk of cross-contamination, and reduces costs. Furthermore, the iPonatic system utilizes one-step rapid nucleic acid release technology, enabling nucleic acid extraction at room temperature without the need for purification. This eliminates the requirement for complex fluidic systems, simplifying the workflow. Nucleic acid extraction, amplification, and detection are fully integrated into a single cartridge, allowing for end-to-end testing with just one sample addition. The cartridge is made from cost-efficient polypropylene injection molding, priced as low as \$0.50, making it highly economical. The system significantly reduces processing time, with nucleic acid extraction completed in just 5 min—compared to 15–30 min for conventional methods. Patients can receive their test reports within 30 min, offering a rapid, cost-effective solution for point-of-care diagnostics. Additionally, the system integrates seamlessly with the Biometa Cloud platform via an equipment service interface, enabling

Research and Development Department, Sansure Biotech Inc., Changsha 410125, China. ✉email: lizhongdai@sansure.com.cn

real-time device status monitoring through a heartbeat mechanism and supporting the real-time uploading of sample information, experimental progress, and results. This integration enables remote management and large-scale data synchronization, providing notable advantages over traditional USB or Bluetooth transmission methods. These enhancements improve the POCT system's suitability for telemedicine and scalable diagnostics.

Experimental validation demonstrated the system's high sensitivity for detecting six pathogens, with limits of detection at 800 copies/mL for three sexually transmitted pathogens and 200 copies/mL for three respiratory pathogens. It also demonstrated excellent accuracy in clinical samples, with all targets achieving an AUC > 0.98, sensitivity exceeding 95%, and specificity of 100%. Compared to existing technologies, this system offers notable advantages in cost-effectiveness, automation, and intelligent features, providing a streamlined solution for rapid infectious disease detection and control.

Materials and methods

Materials

SARS-CoV-2, Influenza Virus and Respiratory Syncytial Virus Multiple Nucleic Acid Diagnostic Kit (PCR-Fluorescence Probing) was supplied by Sansure Biotech Inc (Changsha, China); Chlamydia Trachomatis/Ureaplasma Urealyticum/Neisseria Gonorrhoeae DNA Diagnostic Kit (PCR-Fluorescence Probing) was supplied by Sansure Biotech Inc (Changsha, China); Cell preservation solution (X1004) was supplied by Sansure Biotech Inc (Changsha, China). Data analysis and visualization were conducted using PyCharm 2024.1.6. Schematic illustrations were created with Adobe Illustrator 2025. The instrument and cartridge design were performed using SolidWorks 2021.

Clinical samples

Clinical samples included upper respiratory tract positive and negative samples, as well as sexually transmitted disease positive and negative samples. Upper respiratory tract samples were collected via oropharyngeal and nasal swabs, while sexually transmitted disease samples were collected from cervical swabs. Cervical swabs were preserved in saline solution, and upper respiratory tract samples were preserved in X1004 preservation solution. Samples were transported under low-temperature conditions and stored at $-80\text{ }^{\circ}\text{C}$ until analysis.

The involved clinical specimens were approved by the Ethics Committee of Hunan Provincial People's Hospital (ethics number:2023-26). All methods were carried out in accordance with relevant guidelines and regulations, and informed consent was obtained from all subjects or their legal guardians.

iPonatic real-time fluorescence quantitative PCR protocol

The amplification protocol for the multiplex detection of respiratory pathogens involved reverse transcription at $50\text{ }^{\circ}\text{C}$ for 5 min, initial denaturation at $95\text{ }^{\circ}\text{C}$ for 1 min, followed by 41 cycles of $95\text{ }^{\circ}\text{C}$ for 5 s and $60\text{ }^{\circ}\text{C}$ for 15 s, with a total detection time of approximately 30 min. For the detection of sexually transmitted pathogens, the protocol included initial denaturation at $94\text{ }^{\circ}\text{C}$ for 1 min, followed by 40 cycles of $94\text{ }^{\circ}\text{C}$ for 3 s and $57\text{ }^{\circ}\text{C}$ for 15 s, with a total process time of approximately 23 min.

Statistical analysis

The Receiver Operating Characteristic (ROC) curve was plotted using MedCalc 20.027 (Mariakerke, Belgium) to evaluate the diagnostic ability of the system. Clinical performance is typically assessed using sensitivity and specificity, calculated using the following formulas:

$$SE = \frac{TP}{TP + FN} \times 100\%$$

$$SP = \frac{TN}{TN + FP} \times 100\%$$

SE = Sensitivity; SP = Specificity; TP = True Positive; FN = False Negative; TN = True Negative; FP = False Positive

SLAN-96P real-time PCR protocol

The SLAN-96P real-time PCR system was used as the reference standard, and its detection results were compared with those of the iPonatic system. For oropharyngeal and nasal swab samples, nucleic acid extraction was performed using the Sample Release Reagent (Reference Number: S1014E Series) manufactured by Sansure Biotech Inc., according to the provided protocol. A $10\text{ }\mu\text{L}$ aliquot of the sample was combined with $10\text{ }\mu\text{L}$ of Sample Release Reagent, mixed thoroughly, and incubated at room temperature for 10 min. Subsequently, $20\text{ }\mu\text{L}$ of the extracted RNA was transferred to the PCR tube. To each well, $30\text{ }\mu\text{L}$ of SARS-CoV-2-Flu-RSV-PCR Master Mix was added. The wells were covered, centrifuged at 2000 rpm for 10 s, and then placed into the real-time PCR system. The amplification protocol for SARS-CoV-2, influenza virus, respiratory syncytial virus (RSV), and RNase P detection was as follows: $50\text{ }^{\circ}\text{C}$ for 10 min for reverse transcription, followed by 1 min at $94\text{ }^{\circ}\text{C}$ for denaturation, and 45 cycles of $94\text{ }^{\circ}\text{C}$ for 10 s and $60\text{ }^{\circ}\text{C}$ for 20 s.

For cervical swab samples, $500\text{ }\mu\text{L}$ of the sample was transferred to a 1.5 mL centrifuge tube, and nucleic acid extraction was conducted using the Sample Release Reagent (Lot number: S1013) from Sansure Biotech Inc., following the manufacturer's instructions. In each reaction tube, $38\text{ }\mu\text{L}$ of PCR Master Mix, $2\text{ }\mu\text{L}$ of enzyme mix, and $10\text{ }\mu\text{L}$ of the sample were added. The wells were covered, centrifuged at 2000 rpm for 10 s, and then placed into the real-time PCR system. The amplification protocol for *Chlamydia trachomatis* (CT), *Ureaplasma urealyticum* (UU), *Neisseria gonorrhoeae* (NG), and β -Globin detection was as follows: $50\text{ }^{\circ}\text{C}$ for 2 min for the

UNG enzyme reaction, followed by 5 min at 94 °C for pre-denaturation, and 45 cycles of 94 °C for 15 s and 57 °C for 30 s.

Overview of the design and evaluation of the iPonatic system

In the results section, we first provide a comprehensive overview of the iPonatic system workflow, detailing its innovative design, objectives, and key advantages over conventional detection technologies. We then introduce the quantitative dropper, which integrates sample collection with precise dispensing to streamline operations and enhance detection efficiency. This dropper consists of four main components: a dispensing capsule, tube body, dropper tip, and cap. To evaluate its performance, we conducted an assessment of dispensing accuracy and reproducibility, comparing it with traditional pipetting methods to assess their respective impacts on nucleic acid detection. Next, we describe the detection cartridge's design and operational workflow. The cartridge serves as the core reaction unit of the system, integrating nucleic acid extraction, amplification, and detection into a fully automated process. It comprises four reagent tubes containing the internal control, lysis buffer, reaction buffer, and enzymes, along with a reagent strip carrier, sealing plugs, a filtered pipette tip, a plunger, and a PCR reaction chamber. Once inserted into the system, the cartridge interacts seamlessly with various functional modules, facilitating automated fluid handling, thermal cycling, and real-time fluorescence detection. This integration eliminates the need for manual intervention and reducing the risk of contamination. Finally, we focus on the overall system design. The iPonatic system integrates multiple functional modules, including the reagent strip pushing, vertical motion, pipette pump, PCR, and power modules. The cartridge operates in synergy with these modules, ensuring precise fluid handling and seamless workflow execution. Additionally, we evaluated the thermal control performance of the PCR module and the accuracy of the fluorescence detection module, confirming their stability and reliability in practical applications. This comprehensive system integration shortens turnaround time and improves ease of use, making it well-suited for point-of-care and clinical diagnostics.

Results

Overview of the detection process

The iPonatic system offers a fully integrated, end-to-end workflow that streamlines infectious disease detection, from sample collection to patient report generation, significantly reducing patient waiting time and ensuring faster delivery of results. To accommodate different assay requirements, the system features separate reagent storage, requiring the user to manually load the reagents before testing. This design enhances flexibility and simplifies storage, as reagents are kept individually at low temperatures, reducing transportation costs and maintaining stability. The process consists of four key steps: sample collection (< 1 min) (Fig. 1A), sample loading (< 1 min) (Fig. 1B), sample lysis, amplification and detection (28 min) (Fig. 1C), and result uploading (< 1 min) (Fig. 1D). Conventional workflows for sample loading often rely on manual pipetting, which requires precise handling, operator training, and additional equipments. To address these limitations, the iPonatic system introduces a quantitative dropper. This user-friendly design allows users to simply place a nasal swab into the dropper, which contains the cell preservation solution, and press the dispensing capsule, quickly and accurately transferring the sample into a pre-loaded cartridge. By eliminating the need for pipettes and specialized skills, this streamlined process removes the requirement for additional liquid transfer, thereby reducing preparation time, operational complexity, and associated costs. As a result, the dropper is well-suited for the ideal POCT scenario. Once the cartridge is inserted, the iPonatic system automates nucleic acid extraction using one-step rapid release technology, completing the process in just 5 min. The system then automatically performs amplification and fluorescence detection, requiring no further user intervention.

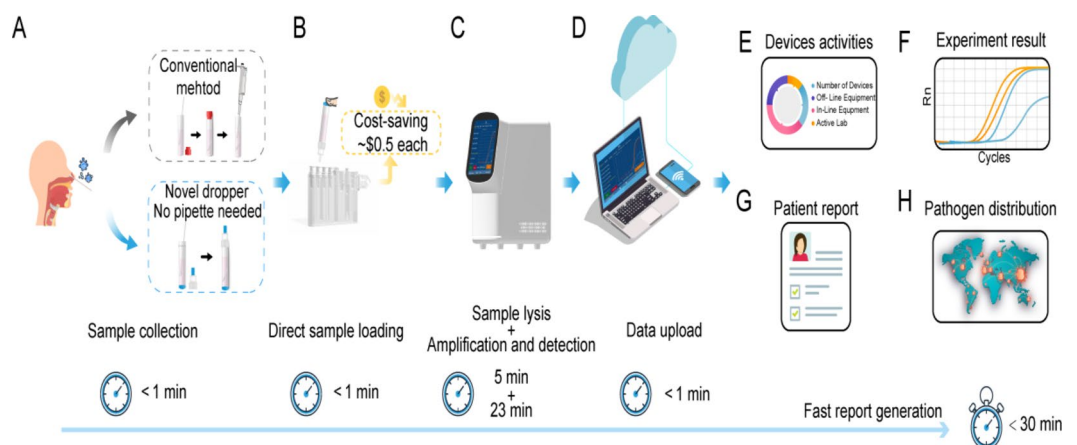


Fig. 1. Overview of the iPonatic system workflow. (A) Sample collection. (B) Direct sample loading using the novel dropper. (C) Sample lysis, amplification and detection. (D) Data upload. (E) Real-time device monitoring. (F) Upload of experimental results. (G) Patient reports generation. (H) Visualization of pathogen distribution.

Integrated with the Biometra Cloud platform, the iPonatic system enables real-time monitoring of device status and experimental progress (Supplementary Fig. S1). During the detection process, the device continuously reports its operating status and experimental data, while a mobile system displays the device's activity and laboratory performance metrics (Fig. 1E, Supplementary Fig. S2). This ensures traceability of the detection workflow and facilitates prompt responses to any anomalies. Upon completion, results are uploaded to the cloud in real time (Fig. 1F, Supplementary Fig. S3), and standardized patient reports are automatically generated, allowing remote physicians to access them instantly (Fig. 1G, Supplementary Fig. S4), significantly reducing diagnostic turnaround time. Moreover, the iPonatic system provides a visual representation of pathogen distribution and dynamic trends (Fig. 1H, Supplementary Fig. S5), delivering valuable insights for infectious disease control and policy decision-making. By completing the entire diagnostic workflow in 30 min, the iPonatic system significantly enhances operational efficiency and minimizes diagnostic delays.

Quantitative dropper design and evaluation

To streamline the detection process and facilitate efficient sample loading, this study developed a quantitative dropper that combines sample collection and controlled dispensing functionalities (Fig. 2A, B). The quantitative dropper consists of four main components: a dispensing capsule, a tube body, a dropper tip, and a cap. The dispensing capsule incorporates a protrusion design that allows for controlled dispensing with a simple press. The tube body features a hollow structure for liquid storage, reinforced with supportive elements to enhance stability and prevent leakage. The angled dropper tip ensures smooth and consistent liquid flow, while a threaded connection improves sealing reliability. The threaded cap further enhances leak prevention and ensures ease of use.

The dropper's performance was systematically evaluated for dispensing accuracy, consistency, and its impact on nucleic acid detection (Fig. 2C). In tests of dispensing accuracy and consistency, four droppers dispensed a preservation solution containing nasal swabs across seven consecutive trials. The results demonstrated stable single dispensing volumes of $20 \pm 5 \mu\text{L}$, meeting the design expectations.

To assess the impact on nucleic acid detection, qPCR tests were conducted for SARS-CoV-2, influenza virus, RSV, and RNase P gene as internal control. The experimental group used $30 \mu\text{L}$ reaction solution and $20 \mu\text{L}$ samples dispensed with the dropper, while the control group used $30 \mu\text{L}$ reaction solution and $20 \mu\text{L}$ samples dispensed with a micropipette (Fig. 2D). Each target was tested in quadruplicate, and no significant

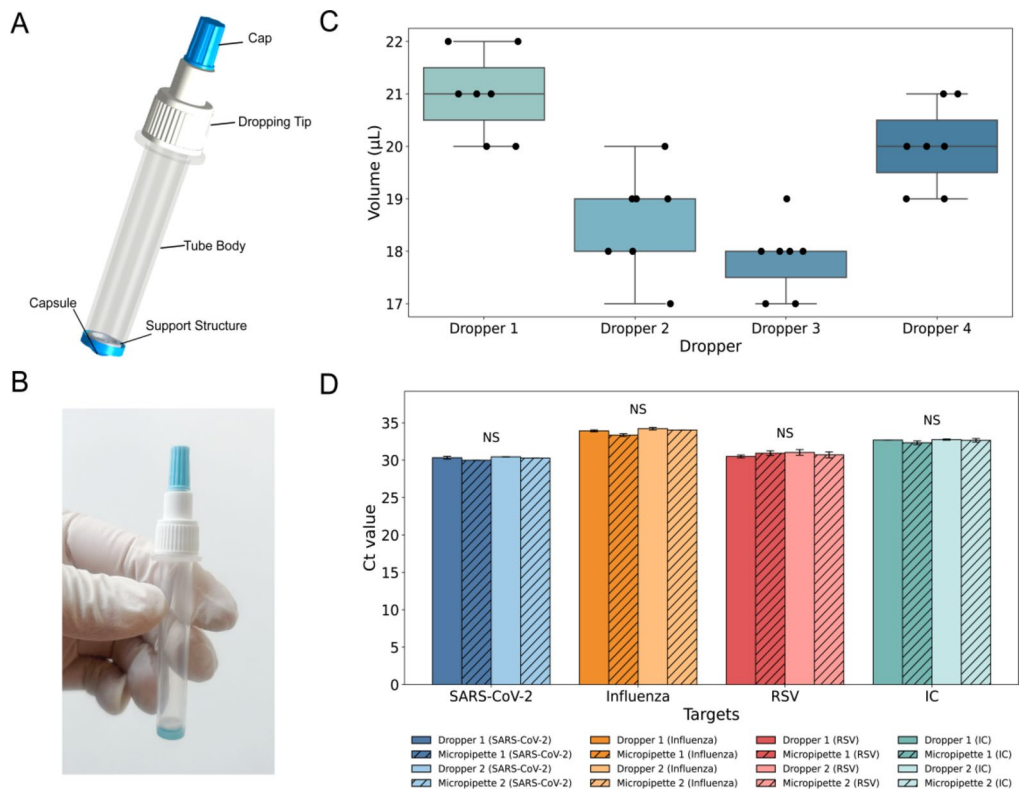


Fig. 2. Design and evaluation of the quantitative dropper. (A) Structural diagram of the quantitative dropper, showing its key components: capsule, tube body with support structure, dropping tip, and cap. (B) Photograph of the actual quantitative dropper prototype. (C) Evaluation of sampling accuracy and consistency across four tested droppers. Error bars represent standard deviation from seven experiments. (D) Comparison of C_t values obtained using the dropper and a pipette in qPCR assays for SARS-CoV-2, influenza, RSV, and RNase P. Error bars represent standard deviation from two experiments. “NS” signifies the absence of a statistically significant difference between the two groups. Error bars represent standard deviation, $n = 2$.

differences in C_t values were observed between the groups, confirming that the dropper ensures accurate and consistent dispensing without affecting detection results. These findings validate the dropper's reliability in terms of dispensing consistency and compatibility with nucleic acid detection. By simplifying sample handling and enabling reliable dispensing, this dropper offers a dependable and efficient solution for POCT workflows.

Cartridge design and workflow

This study developed a disposable detection cartridge that fully automates the workflow for sample processing and PCR reactions. Leveraging a one-step rapid nucleic acid release technology, the cartridge enables sample lysis at room temperature, eliminating the need for complex nucleic acid extraction. This significantly reduces sample processing time and simplifies operation. The cartridge design incorporates four reagent tubes storing the internal control, lysis buffer, reaction buffer, and enzymes, along with a reagent strip carrier, sealing plugs, a pipette tip with a filter, a plunger, and a PCR reaction chamber (Fig. 3A, B). The system employs a liquid-handling pump with disposable filtered pipette tips to automate reagent transfer and mixing. A plunger dispenses the mixed reagents into the PCR reaction chamber and creates an isolated, sealed environment with a venting channel to prevent aerosol contamination and liquid evaporation.

The sample loading and reaction preparation process involves the following steps: First, the user adds the sample to the lysis buffer tube (Tube 2)) for lysis (Fig. 3C). The pump then transfers the reaction buffer (Tube 3) into the enzyme reaction buffer (Tube 4) and mixes them thoroughly (Fig. 3D). The resulting mixture is transferred to the PCR loading port (Port 8)) (Fig. 3E). The internal control (Tube 1)) and lysed sample solution (Tube 2)) are then sequentially transferred to the PCR loading port and mixed (Figs. 3F, G). Finally, the plunger (Port 7)) injects the mixture into the PCR reaction chamber, completing the reaction setup (Fig. 3H). Once prepared, the reagents in the PCR reaction chamber are ready for amplification and detection. This highly automated and integrated design minimizes manual intervention, streamlines the workflow, and significantly enhances the efficiency of nucleic acid testing.

System design and thermal–optical characterization

The iPontic system integrates the reagent strip pushing module, vertical motion module, pipette pump module, PCR module, and power module (Fig. 4A), supporting the full automation of sample distribution, nucleic

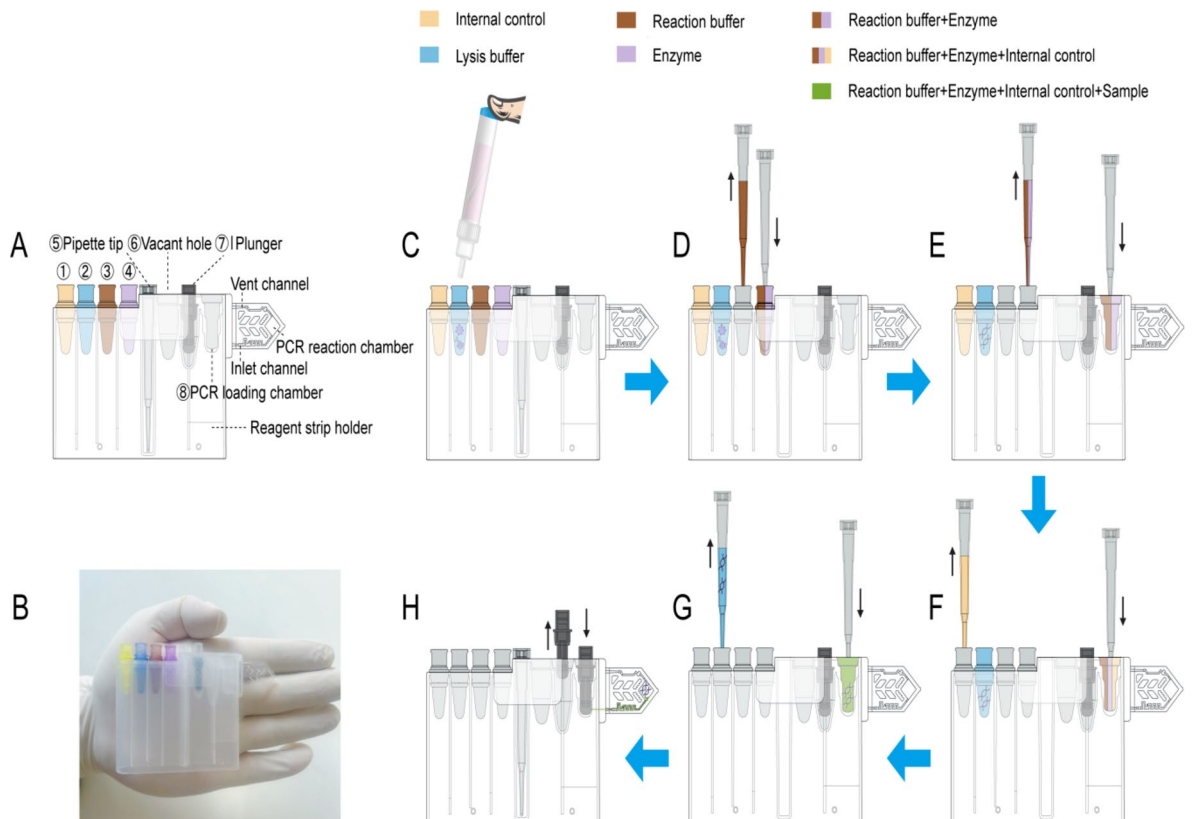


Fig. 3. Cartridge design and workflow. (A) Structural diagram of the cartridge. (B) Photograph of the cartridge. (C–H) Reaction workflow: (C) Sample addition to the lysis buffer tube for nucleic acid release. (D) Mixing of reaction buffer with the enzyme. (E) Transfer of the mixed solution to the PCR loading chamber. (F) Addition and mixing of internal control in the PCR loading chamber. (G) Addition and mixing of lysed sample in the PCR loading chamber. (H) Injection of the final mixture into the PCR reaction chamber using the plunger for amplification and detection.

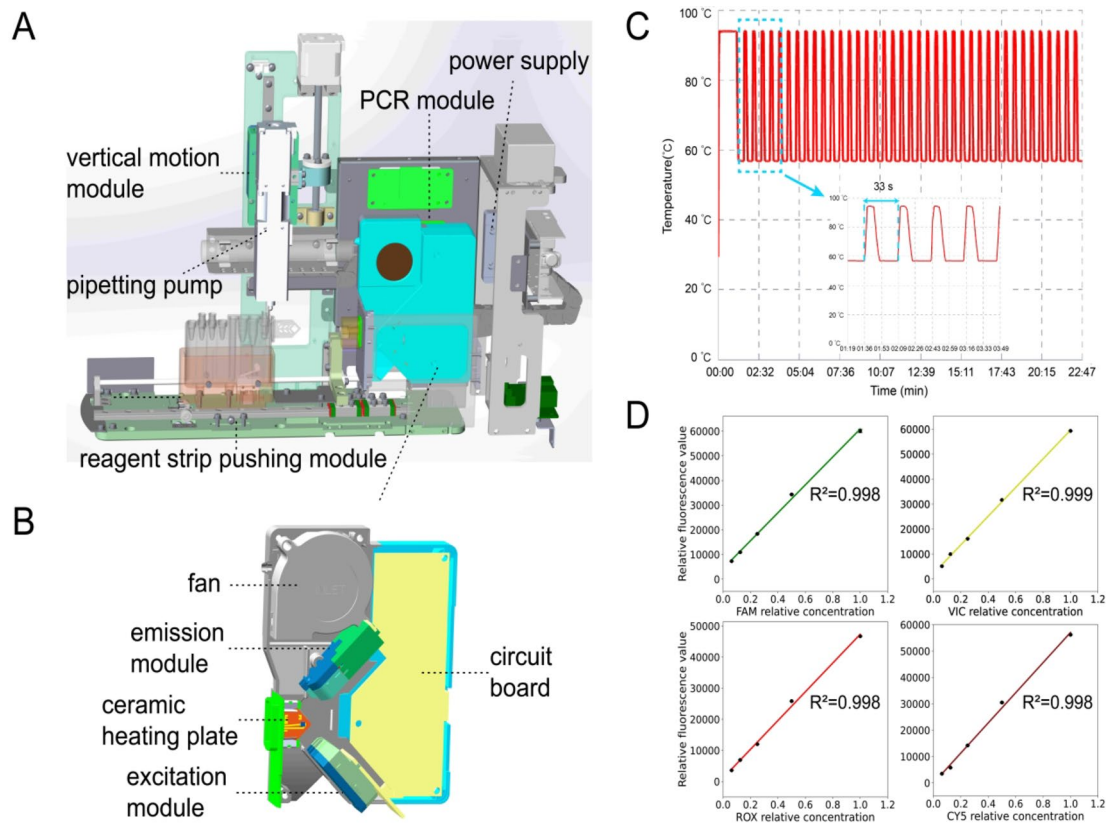


Fig. 4. System design and thermal-optical characterization. **(A)** Schematic diagram of the nucleic acid detection system, showing the integrated modules: reagent strip pushing module, vertical motion module, pipetting pump module, PCR module, and power supply module. **(B)** Structural layout of the PCR module, including the circuit board, ceramic heating plate, excitation module, emission module, and fan. **(C)** Temperature profile during 40 thermal cycles in the PCR chamber. **(D)** Linearity of the fluorescence detection module across four channels (FAM, VIC, ROX, CY5) using gradient-diluted standard fluorescent dyes.

acid lysis, PCR amplification and detection. The core of the system is the PCR module, which includes a rapid temperature control module and a four-channel fluorescence detection module (Fig. 4B). The temperature control module combines ceramic heating plates and high-speed fans for rapid and stable temperature regulation. The ceramic plates' low thermal resistance and high efficiency allow quick heating, while the high-speed fan with a hyperbolic throat structure significantly enhances cooling efficiency. Additionally, the integrated Proportional-Integral-Derivative (PID) temperature control algorithm and high-precision temperature sensors further guarantee the accuracy and stability of temperature control. Performance validation shows that the PCR module successfully completes 40 thermal cycles in 22 min at room temperature (20 °C) using a program targeting sexually transmitted infection pathogens, proving the stability and efficiency of the thermal system (Fig. 4C).

The fluorescence detection module includes an excitation module and an emission module, arranged at a 90° angle to the reagent strip, with support for four fluorescence channels: FAM, VIC, ROX, and CY5 (Supplementary Fig. S6, Supplementary Table S1). The excitation light sources are high-efficiency LEDs, with the optical path fine-tuned by lenses, mirrors, and a dichroic mirror to excite the fluorophores. The emission path captures the fluorescence signal and outputs the fluorescence intensity through optical filters and a photoconversion module. Performance evaluation involved testing a series of gradient-diluted standard fluorescent dyes, collecting 10 signal points at each concentration. Results showed a strong linear correlation ($R^2 > 0.99$) across all four channels, demonstrating the module's high accuracy and reliability in signal quantification (Fig. 4D).

Detection performance evaluation

To evaluate the system's diagnostic performance, we conducted comprehensive testing for eight targets, including sexually transmitted pathogens: CT, UU, NG, with β -Globin as the internal control, as well as respiratory pathogens: SARS-CoV-2, influenza, RSV, with RNase P as the internal control. First, we compared the results of the iPonatic system with those from the SLAN-96P Real-Time PCR system by testing different concentrations of sexually transmitted pathogen control samples (Fig. 5A–D). To further evaluate the agreement between the two methods, a Bland-Altman plot was generated (Fig. S8). The C_t values measured by the iPonatic system for CT, UU, NG, and β -Globin were highly consistent with those obtained from the SLAN-96P Real-Time PCR system, confirming the accuracy and reliability of the iPonatic system.

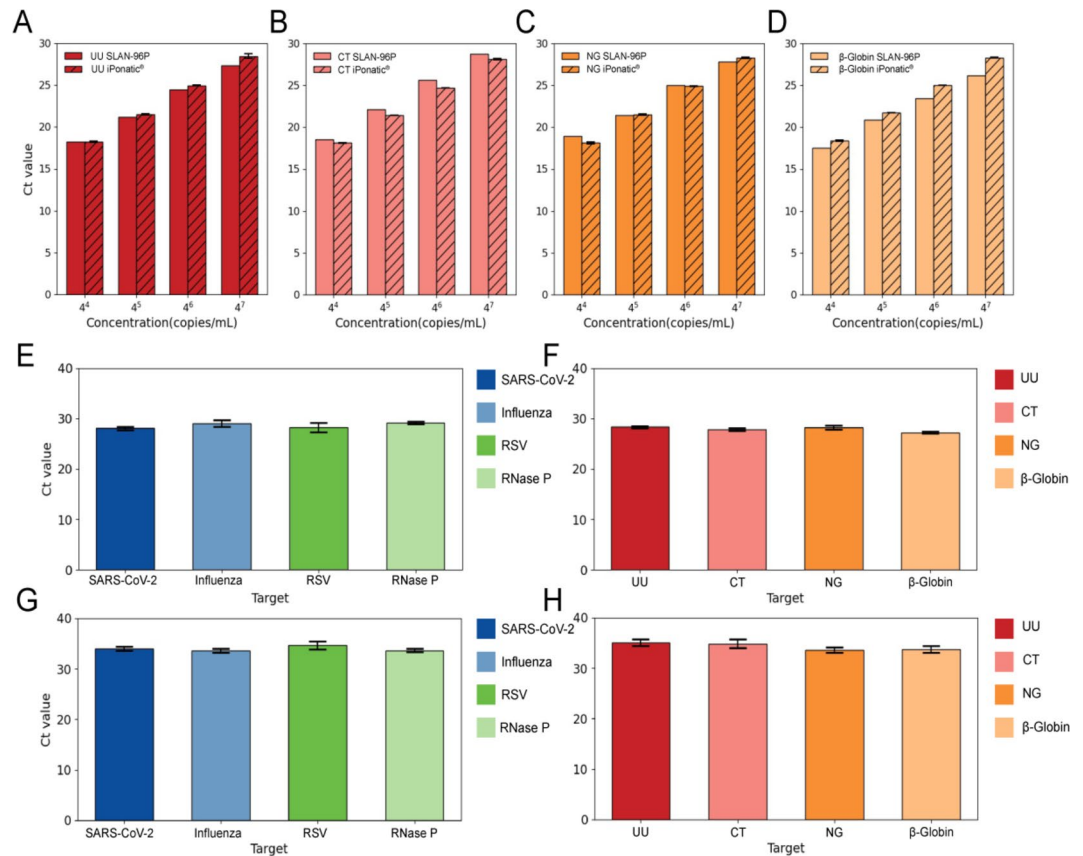


Fig. 5. Performance evaluation of the iPonatic system. (A–D) Comparison of *Ct* values at different concentrations for (A) UU, (B) CT, (C) NG and (D) β-Globin between the iPonatic system and the SLAN-96P system. (E, F) Sensitivity evaluation across 10 repeated tests for all targets. (E) Bar plots of *Ct* values for respiratory pathogens at 200 copies/mL. (F) Bar plots of *Ct* values for sexually transmitted pathogens at 800 copies/mL. (G, H) Precision evaluation across 10 repeated tests for all targets. (G) Bar plots of *Ct* values for respiratory pathogens at 1.00×10^5 copies/mL. (H) Bar plots of *Ct* values for sexually transmitted pathogens at 2.00×10^5 copies/mL.

Next, we evaluated the system's detection sensitivity. For respiratory pathogens, we diluted the control samples of SARS-CoV-2, influenza, RSV, and RNase P to a theoretical concentration of 200 copies/mL and tested each target 10 times. For sexually transmitted pathogens, we diluted the control samples of CT, UU, NG, and β-Globin to 800 copies/mL, with each target tested 10 times. The results showed stable *Ct* values across all targets, with a 100% detection rate (Fig. 5E, F). To assess the system's precision, we conducted repeated tests on control samples for both respiratory and sexually transmitted pathogens, diluted to 1.00×10^5 copies/mL and 2.00×10^5 copies/mL respectively, with each target tested 10 times. The coefficient of variation for all detection channels was below 5%, demonstrating the system's reliable stability and precision in detecting both types of pathogens (Fig. 5G, H). The iPonatic system exhibits high accuracy, sensitivity, and precision in multi-target detection, underscoring its potential for clinical pathogen diagnostics.

Diagnostic accuracy assessment

To evaluate the clinical applicability of the iPonatic system for infectious disease screening, we tested 420 cervical swab samples and 739 respiratory samples, targeting sexually transmitted pathogens (CT, UU, NG) with β-Globin as the internal control, and respiratory pathogens (SARS-CoV-2, influenza, and RSV) with RNase P as the internal control. All internal controls were positive, confirming the reliability of the sample quality. In comparison to the SLAN-96P Real-Time PCR system, we found that only 2 SARS-CoV-2-positive and 8 influenza-positive samples tested negative on the iPonatic system. All other results showed complete agreement between the iPonatic and the SLAN-96P system (Figs. 6A, B, S9). ROC curve analysis showed that the AUC values for all targets exceeded 0.98 (Fig. 6C–H), validating the system's outstanding diagnostic capability in multi-target detection.

For sexually transmitted pathogens (CT, UU, and NG), no false positives or false negatives were observed, with both sensitivity and specificity reaching 100.0% (sensitivity 95% CI: 95.5–100.0%; specificity 95% CI: 97.4–100.0%) (Table 1). For respiratory pathogens, the sensitivity of SARS-CoV-2 and influenza exceeds 95%, with specificity at 100.0%; the sensitivity and specificity for RSV were both 100.0% (Table 2). These results further

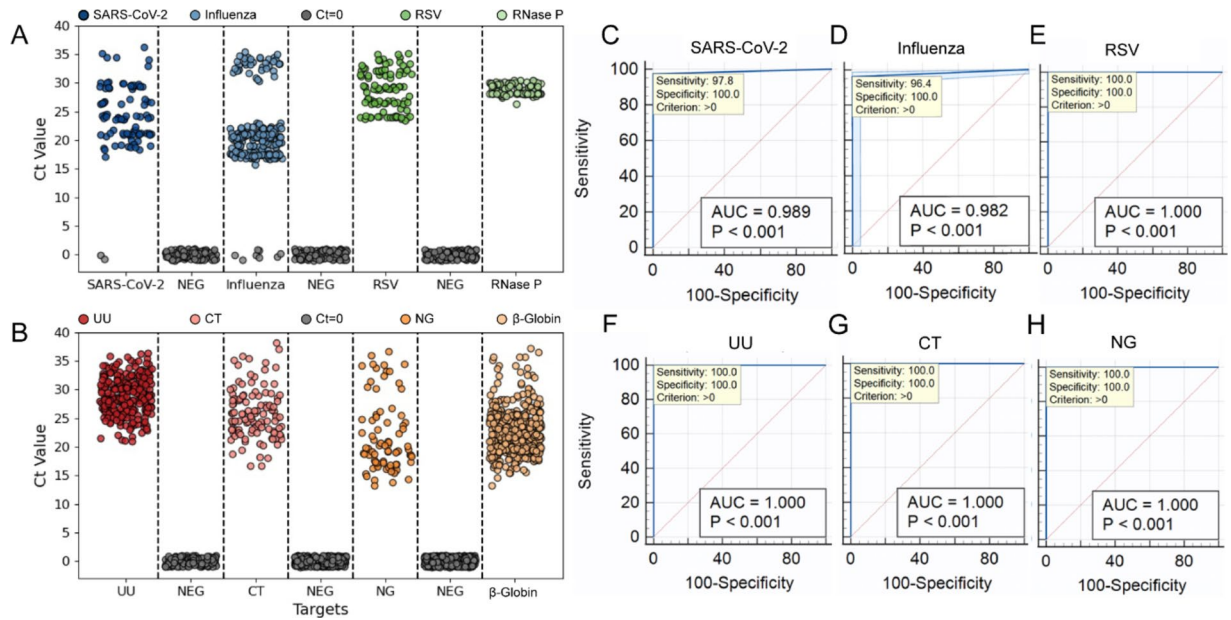


Fig. 6. Clinical performance evaluation of the iPonatic system. (A, B) *Ct* value distribution of (A) SARS-CoV-2, influenza virus, RSV, RNase P for respiratory samples and (B) UU, CT, NG, β-Globin for cervical swab samples by the iPonatic system. (C–E) ROC curves for (C) SARS-CoV-2, (D) influenza virus, (E) RSV. (F–H) ROC curves for (F) UU, (G) CT, (H) NG.

Target	Total specimens	TP ^a	FP ^b	TN ^c	FN ^d	Sensitivity (95% CI) ^e	Specificity (95% CI) ^e
<i>Chlamydia trachomatis</i>	420	112	0	308	0	100% (96.8–100.0%)	100% (98.8–100.0%)
<i>Ureaplasma urealyticum</i>	420	279	0	141	0	100% (98.7–100.0%)	100% (97.4–100.0%)
<i>Neisseria gonorrhoeae</i>	420	80	0	340	0	100% (95.5–100.0)	100% (98.9–100.0%)

Table 1. Detection accuracy of sexually transmitted pathogen of the iPonatic system. ^aTrue positive. ^bFalse positive. ^cTrue negative. ^dFalse negative. ^eConfidence interval.

Target	Total specimens	TP ^a	FP ^b	TN ^c	FN ^d	Sensitivity (95% CI) ^e	Specificity (95% CI) ^e
SARS-CoV-2	197	87	0	108	2	97.75% (92.1–99.7%)	100% (96.6–100.0%)
Influenza	330	214	0	108	8	96.4% (93.0–98.4%)	100% (96.6–100.0%)
RSV	207	99	0	108	0	100% (96.3–100.0%)	100% (96.6–100.0%)

Table 2. Detection accuracy of respiratory pathogens of the iPonatic system. ^aTrue positive. ^bFalse positive. ^cTrue negative. ^dFalse negative. ^eConfidence interval.

confirm the high reliability and accuracy of the system in screening for respiratory and sexually transmitted pathogens.

Discussion

This study presents the development of the iPonatic system, a fully integrated POCT solution designed to address critical challenges in infectious disease diagnostics. By incorporating a quantitative dropper for sample handling, one-step nucleic acid release technology for rapid sample processing, and cloud-based data synchronization for real-time reporting, the system bridges significant gaps in speed, accessibility, and efficiency. Completing the entire diagnostic workflow in 30 min, the iPonatic system drastically reduces patient waiting time, streamlines healthcare delivery, and supports telemedicine applications. These features position the system as an ideal solution for decentralized, scalable, and patient-centered diagnostics, particularly in resource-limited settings, while improving diagnostic equity and enhancing overall patient care.

Compared to conventional nucleic acid extraction techniques such as magnetic bead- or column-based methods, the one-step nucleic acid release technology used in the iPonatic system eliminates complex fluidic systems and reduces processing time. With just a single sample addition, the system completes the entire testing process, streamlining operations and enhancing user convenience. This aligns with prior research emphasizing

the importance of minimizing procedural steps to increase accessibility in point-of-care applications^{3,4,24}. Additionally, the system's quantitative dropper eliminates the need for pipettes and technical expertise, addressing a critical bottleneck in POCT usability and reducing the risk of cross-contamination. Real-time epidemic mapping, integrated through cloud-based technology, further distinguishes the iPonatic system from existing solutions by providing actionable insights for data-driven surveillance and public health decision-making.

For sexually transmitted infections, this study primarily evaluated cervical specimens as a proof-of-concept due to their widespread use in clinical diagnostics. However, real-world POCT scenarios often involve a broader range of specimen types, including vaginal swabs, penile swabs, and urine, which offer more patient-friendly and non-invasive collection options. Future studies should assess the feasibility and validation of these alternative sample types to ensure broader clinical applicability. Notably, since the iPonatic system does not incorporate a nucleic acid purification step, urine samples may not be suitable for direct testing due to the presence of inhibitory components such as urea and nucleases, which could interfere with the PCR reaction. Further evaluation is needed to determine appropriate processing strategies. Additionally, due to specimen availability constraints, this study utilized stored clinical samples rather than freshly collected POCT specimens. While stored samples provided a controlled testing environment, future validation with fresh clinical specimens is needed to better reflect real-world POCT performance.

To meet varying detection needs, we also designed a “smart all-in-one machine” capable of flexibly connecting 1 to 8 detection modules (Supplementary Fig. S7). This design allows users to select the appropriate number of modules based on the application scenario, and the system is centrally controlled through an integrated intelligence platform, with results displayed directly on the smart all-in-one machine screen. This flexibility provides diverse solutions for high-throughput or specialized testing needs.

Although the system demonstrates strong performance in nucleic acid testing, there is still potential for further optimization. For instance, incorporating melting curve analysis²⁵ or adding additional fluorescence channels could expand its multi-target detection capabilities. Furthermore, the system's open architecture allows for compatibility with various sample preparation reagents, offering the flexibility to incorporate emerging pathogens and antimicrobial resistance markers, thereby broadening its clinical applications. By integrating multiple nucleic acid amplification techniques—such as LAMP, RPA and CRISPR²⁶—the system could be enhanced to address a wider range of diagnostic needs, further strengthening its clinical utility.

Conclusion

In this work, we developed the iPonatic system that combines a quantitative dropper, low-cost cartridges utilizing one-step rapid nucleic acid release technology, and cloud-based data synchronization, enabling fast report generation and significantly reducing patient waiting time. The system's performance was validated by testing six key pathogens: CT, UU, NG, SARS-CoV-2, influenza virus, and RSV. The detection results demonstrated a high degree of consistency with standard real-time quantitative PCR instruments. The test results were obtained in 30 min, with a lower detection limit of 200 copies/mL for respiratory pathogens and 800 copies/mL for sexually transmitted pathogens. Testing of 420 cervical and 739 respiratory samples further confirmed the system's diagnostic accuracy. ROC analysis showed AUC values greater than 0.98 for all targets. Sensitivity and specificity for sexually transmitted pathogens were 100%, while sensitivity for respiratory pathogens exceeded 95%, with specificity reaching 100%. With its rapid, cost-effective, and efficient design, this system is particularly well-suited for grassroots healthcare, epidemic response, and public health management, especially in resource-limited settings or for high-throughput screening applications.

Data availability

The authors declare that the data supporting the findings of this study are available within the paper, the supplementary information file, and from the corresponding author upon reasonable request.

Received: 26 January 2025; Accepted: 2 April 2025

Published online: 21 April 2025

References

- Safiabadi, T. et al. Tools and techniques for severe acute respiratory syndrome coronavirus 2 (SARS-CoV-2)/COVID-19 detection. *Clin. Microbiol. Rev.* **34**, 20. <https://doi.org/10.1128/cmr.00228-20> (2021).
- Schmitz Jonathan, E., Stratton Charles, W., Persing David, H. & Tang, Y. W. Forty years of molecular diagnostics for infectious diseases. *J. Clin. Microbiol.* **60**, e02446. <https://doi.org/10.1128/jcm.02446-21> (2022).
- Nelson, P. P. et al. Current and future point-of-care tests for emerging and new respiratory viruses and future perspectives. *Front. Cell. Infect. Microbiol.* **10**. <https://doi.org/10.3389/fcimb.2020.00181> (2020).
- Land, K. J., Boeras, D. I., Chen, X. S., Ramsay, A. R. & Peeling, R. W. REASSURED diagnostics to inform disease control strategies, strengthen health systems and improve patient outcomes. *Nat. Microbiol.* **4**, 46–54. <https://doi.org/10.1038/s41564-018-0295-3> (2019).
- Shrivastava, S., Trung, T. Q. & Lee, N. E. Recent progress, challenges, and prospects of fully integrated mobile and wearable point-of-care testing systems for self-testing. *Chem. Soc. Rev.* **49**, 1812–1866. <https://doi.org/10.1039/C9CS00319C> (2020).
- Maffert, P., Reverchon, S., Nasser, W., Rozand, C. & Abaibou, H. New nucleic acid testing devices to diagnose infectious diseases in resource-limited settings. *Eur. J. Clin. Microbiol. Infect. Dis.* **36**, 1717–1731. <https://doi.org/10.1007/s10096-017-3013-9> (2017).
- Drancourt, M., Michel-Lepage, A., Boyer, S. & Raoult, D. The point-of-care laboratory in clinical microbiology. *Clin. Microbiol. Rev.* **29**, 429–447. <https://doi.org/10.1128/cmr.00090-15> (2016).
- Mabey, D., Peeling, R. W., Ustianowski, A. & Perkins, M. D. Diagnostics for the developing world. *Nat. Rev. Microbiol.* **2**, 231–240. <https://doi.org/10.1038/nrmicro841> (2004).
- Wang, S. et al. Advances in addressing technical challenges of point-of-care diagnostics in resource-limited settings. *Expert Rev. Mol. Diagn.* **16**, 449–459. <https://doi.org/10.1586/14737159.2016.1142877> (2016).

10. Shaw, J. L. V. Practical challenges related to point of care testing. *Pract. Lab. Med.* **4**, 22–29. <https://doi.org/10.1016/j.plabm.2015.12.002> (2016).
11. Mosley, O. et al. Sample introduction interface for on-chip nucleic acid-based analysis of *Helicobacter pylori* from stool samples. *Lab. Chip*. **16**, 2108–2115. <https://doi.org/10.1039/C6LC00228E> (2016).
12. Czilwik, G. et al. Rapid and fully automated bacterial pathogen detection on a centrifugal-microfluidic labdisk using highly sensitive nested PCR with integrated sample Preparation. *Lab. Chip*. **15**, 3749–3759. <https://doi.org/10.1039/C5LC00591D> (2015).
13. Petralia, S., Sciuto, E. L. & Conoci, S. A novel miniaturized biofilter based on silicon micropillars for nucleic acid extraction. *Analyst* **142**, 140–146. <https://doi.org/10.1039/C6AN02049F> (2017).
14. Jangam, S. R., Agarwal, A. K., Sur, K. & Kelso, D. M. A point-of-care PCR test for HIV-1 detection in resource-limited settings. *Biosens. Bioelectron.* **42**, 69–75. <https://doi.org/10.1016/j.bios.2012.10.024> (2013).
15. Han, K., Yoon, Y. J., Shin, Y. & Park, M. K. Self-powered switch-controlled nucleic acid extraction system. *Lab. Chip* **16**, 132–141. <https://doi.org/10.1039/C5LC00891C> (2016).
16. Liu, T. et al. Fingerprint blood-based nucleic acid testing on a USB interfaced device towards HIV self-testing. *Biosens. Bioelectron.* **209**, 114255. <https://doi.org/10.1016/j.bios.2022.114255> (2022).
17. Zhu, H. et al. IoT PCR for pandemic disease detection and its spread monitoring. *Sens. Actuators B Chem.* **303**, 127098. <https://doi.org/10.1016/j.snb.2019.127098> (2020).
18. Jain, S. et al. Internet of medical things (IoMT)-integrated biosensors for point-of-care testing of infectious diseases. *Biosens. Bioelectron.* **179**, 113074. <https://doi.org/10.1016/j.bios.2021.113074> (2021).
19. Liu, J., Geng, Z., Fan, Z., Liu, J. & Chen, H. Point-of-care testing based on smartphone: the current state-of-the-art (2017–2018). *Biosens. Bioelectron.* **132**, 17–37. <https://doi.org/10.1016/j.bios.2019.01.068> (2019).
20. Boehme Catharina, C. et al. Rapid molecular detection of tuberculosis and Rifampin resistance. *N. Engl. J. Med.* **363**, 1005–1015. <https://doi.org/10.1056/NEJMoa0907847>
21. Piatek, A. S. et al. GeneXpert for TB diagnosis: planned and purposeful implementation. *Glob. Health Sci. Pract.* **1**. <https://doi.org/10.9745/GHSP-D-12-00004> (2013).
22. Huang, H. S. et al. Multiplex PCR system for the rapid diagnosis of respiratory virus infection: systematic review and meta-analysis. *Clin. Microbiol. Infect.* **24**, 1055–1063. <https://doi.org/10.1016/j.cmi.2017.11.018> (2018).
23. Li, Z. et al. Fully integrated microfluidic devices for qualitative, quantitative and digital nucleic acids testing at point of care. *Biosens. Bioelectron.* **177**, 112952. <https://doi.org/10.1016/j.bios.2020.112952> (2021).
24. Soin, N., Fishlock, S. J., Kelsey, C. & Smith, S. Triboelectric effect enabled self-powered, point-of-care diagnostics: opportunities for developing assured and reassured devices. *Micromachines* **12**, 1 (2021).
25. Yu, Y. et al. Multiplex digital PCR with digital melting curve analysis on a self-partitioning slipchip. *Analyst* **147**, 625–633. <https://doi.org/10.1039/d1an01916c> (2022).
26. Craw, P. & Balachandran, W. Isothermal nucleic acid amplification technologies for point-of-care diagnostics: a critical review. *Lab. Chip*. **12**, 2469–2486. <https://doi.org/10.1039/C2LC40100B> (2012).

Acknowledgements

This research was financially supported by the Central Guidance Local Special Funds, China (2024ZYC031) and the Joint Funds of the National Natural Science Foundation of China (2024JJ9151).

Author contributions

Y.P.X. and L.Z.D. contributed to designing the study. L.C.W., C.W., C.W.Y., J.J.L. and J.G.L. performed the experiments. Y.Y., S.W.H., L.C.W., C.W., C.W.Y., J.J.L. and J.G.L. analyzed data and prepared figures. Y.P.X. and L.Z.D. conceived and supervised the study. Y.Y., S.W.H., and Y.P.X. drafted the manuscript. All authors participated in manuscript editing and approved the manuscript.

Declarations

Competing interests

The authors declare no competing interests.

Additional information

Supplementary Information The online version contains supplementary material available at <https://doi.org/10.1038/s41598-025-97155-4>.

Correspondence and requests for materials should be addressed to L.D.

Reprints and permissions information is available at www.nature.com/reprints.

Publisher's note Springer Nature remains neutral with regard to jurisdictional claims in published maps and institutional affiliations.

Open Access This article is licensed under a Creative Commons Attribution-NonCommercial-NoDerivatives 4.0 International License, which permits any non-commercial use, sharing, distribution and reproduction in any medium or format, as long as you give appropriate credit to the original author(s) and the source, provide a link to the Creative Commons licence, and indicate if you modified the licensed material. You do not have permission under this licence to share adapted material derived from this article or parts of it. The images or other third party material in this article are included in the article's Creative Commons licence, unless indicated otherwise in a credit line to the material. If material is not included in the article's Creative Commons licence and your intended use is not permitted by statutory regulation or exceeds the permitted use, you will need to obtain permission directly from the copyright holder. To view a copy of this licence, visit <http://creativecommons.org/licenses/by-nc-nd/4.0/>.

© The Author(s) 2025